Revisiting a Proposed Kinetic Model for the Reaction of Cysteine and Hydrogen Peroxide via Cysteine Sulfenic Acid

MICHAEL T. ASHBY, PÉTER NAGY

Department of Chemistry and Biochemistry, University of Oklahoma, Norman, OK 73019

Received 29 April 2006; revised 11 July 2006; accepted 21 July 2006

DOI 10.1002/kin.20211
Published online in Wiley InterScience (www.interscience.wiley.com).

ABSTRACT: A mechanism for the oxidation of cysteine by hydrogen peroxide has been proposed by Luo et al. (J *Pharm Sci*, 2005, 94, 304–316): rapid equilibrium to form cysteinate (CS^-), followed by irreversible oxidation of CS^- by H_2O_2 to give cysteine sulfenic acid (CSOH), and nucleophilic attack on CSOH by CS^- to yield cystine (CSSC). We have argued that the data that were published by Luo et al. afford no insight into the mechanism that follows the rate-limiting step, oxidation of CS^- by H_2O_2 (J *Pharm Sci*, 2006, 95, 15–18), but Anderson and Luo contend that their model is sound (J *Pharm Sci*, 2006, 95, 19–24). Evidence is presented herein that discredits the model proposed by Luo et al.: (1) time-resolved ^{1}H NMR spectra show that no intermediate is produced, (2) time-resolved electronic spectra exhibit multiple isosbestic points, and (3) kinetic measurements and models employ the initial rate method (which focus on that part of the kinetic traces for which the differences between the two models are most pronounced). All three experiments verify that a pseudo-first-order model with a single kinetic parameter completely describes the observed kinetics of the oxidation of CS^- by H_2O_2. © 2006 Wiley Periodicals, Inc. Int J Chem Kinet 39: 32–38, 2007

INTRODUCTION

Cysteine is one of the least frequently employed amino acids in biosynthesis [1], presumably due in part to its reactivity relative to other amino acids, particularly with respect to oxidation. However, it is this reactivity that is exploited by many defensive mechanisms for oxidative stress. Nonetheless, the reactivity of the sulfhydryl group can be burdensome when reactive sulfur species [2–4] are formed. While the one electron oxidation of cysteine (CSH) to form cystine (CSSC) is

Correspondence to: Michael T. Ashby; e-mail: mashby@ou.edu.
Contract grant sponsor: American Heart Association.
Contract grant number: 0555677Z.
Contract grant sponsor: National Science Foundation.
Contract grant number: CHE-0503984.
Contract grant sponsor: National Institutes of Health.
Contract grant number: 5 P20 RR018741-02.
Contract grant sponsor: Petroleum Research Fund.
Contract grant number: 42850-AC4.

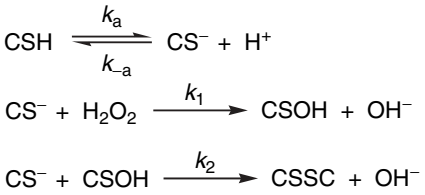

Scheme 1 Mechanism for the reaction of cysteine with hydrogen peroxide as proposed by Luo et al.

an enzymatically reversible process, the two electron oxidation of CSH to give cysteine sulfenic acid (CSOH) is potentially problematic. Analysis of kinetic data for the oxidation of CSH by hydrogen peroxide (H_2O_2) to give CSSC led Luo et al. to propose the mechanism shown in Scheme 1 [5]. This is the same mechanism that has been suggested (or implied) by others [6–8]. The value of k_1 is not in dispute; however, Luo et al. have suggested that they have also measured a rate constant for the second step of the mechanism (k_2), the reaction of CSOH with CS^- to give CSSC [5,9]. If correct, this would be a significant achievement since there are apparently no other reactions of CSOH for which kinetic measurements have been possible. Upon close scrutiny of the evidence that was presented in the original study [5], we have concluded that the data of Luo et al. do not rule out a simpler rate law that excludes the second, faster step of the reaction, the reaction of CSOH with CS^- to give CSSC [10]. While citing statistical evidence to support their position, Anderson and Luo adamantly disagreed with our assessment [9]. Since no new data were offered in either our comment [10] or the response by Anderson and Luo [9], the issue apparently remains unresolved. As for all theories, reaction mechanisms cannot be proven, but a preponderance of evidence can support the theory, or in some cases it is possible to disprove a theory with experiments. We do not believe in the present case there exists overwhelming evidence in support of, nor experimental evidence that disproves, either of the two models. Mechanisms can be supported (or disproved) by kinetic and/or extrakinetic methods. Rate laws by themselves rarely unambiguously evidence a reaction mechanism. Extrakinetic methods include the isolation and/or characterization of a putative reaction intermediate. Kinetic and extrakinetic methods are employed herein to demonstrate that the rate law that was proposed by Luo et al. is incorrect.

EXPERIMENTAL

Reagents

Water was doubly distilled in glass. L-Cystine, L-cysteine, L-cysteic acid monohydrate, L-cysteinesulfinic acid monohydrate, H_2O_2 (30 wt% in water), deuterium chloride (35 wt% solution in D_2O), sodium 3-(trimethylsilyl)-1-propanesulfonate, and K_3PO_4 were used as received from Sigma-Aldrich (St. Louis, MO). $Na_3PO_4 \cdot 12H_2O$ was used as received from Mallinckrodt (Paris, KY). Deuterium oxide (99.9%) was obtained from Cambridge Isotope Laboratories (Andover, MA). L-Cystine *S*-monoxide was synthesized using methods that have been previously described [11]. The concentrations of stock solutions of H_2O_2 were determined iodometrically. The concentration of H_2O_2 in solutions that were prepared from the stock solution of H_2O_2 was confirmed spectrophotometrically ($\varepsilon(H_2O_2)_{240\,nm} = 36.5\ M^{-1}cm^{-1}$).

pH/pD Measurements

pH measurements were made with an Orion ion analyzer EA920 using a Ag/AgCl combination pH electrode. pD measurements in D_2O were made using the same pH electrode by adding 0.41 units to the measurement.

NMR Studies

^1H NMR spectra were recorded with a Varian XL-300 spectrometer at 298.0 (±0.5) K. Deuterated buffers were prepared from D_2O solutions of anhydrous K_3PO_4 by adding DCl. The chemical shifts (ppm) were referenced to sodium 3-(trimethylsilyl)-1-propanesulfonate (DSS, $\delta = 0.015$ ppm). A hand mixer consisting of two Hamilton syringes and a T-mixer was employed to rapidly mix solutions of CSH with solutions of H_2O_2, and ^1H NMR data collection was initiated within 30 s of mixing of the solutions. Transient spectra were averaged to achieve the desired signal/noise. For the spectrum of Fig. 2 that was collected during the initial chemical reaction of CSH and H_2O_2, 16 transients were averaged. Following completion of the initial reaction between CSH and H_2O_2 to largely yield CSSC, data collection was continued for 8 h, with transient spectra collected every hour (average of 128 transients) to establish whether subsequent reactions were observed. The transient spectra were analyzed by comparing the observed spectra with standard samples of L-cystine, L-cysteine, L-cysteic acid, L-cysteinesulfinic acid, and L-cystine *S*-monoxide. The time-resolved spectra were integrated with respect to the internal standard DSS to achieve mass balance of all of the cysteine-derived species.

UV Spectroscopy

Reference UV–visible spectra were measured using an HP 8452A diode array spectrophotometer or the

MOS-450 monochromator of a Bio-Logic stopped-flow instrument using a Xe arc lamp and a PMT detector. Time-resolved UV–visible spectra were recorded using the HP 8452A diode array spectrophotometer in kinetic mode. The latter reactions were initiated using a hand mixer (described earlier) and a flow cell with a 1-cm pathlength or the same hand mixer and a conventional cell with a 1-mm pathlength. Spectral data were analyzed using SPECFIT/32 (Spectrum Software Associates), a multivariate data analysis program.

Stopped-Flow Studies

Kinetic measurements were made with a Bio-Logic instrument that consists of an SFM-400/Q triple mixer, an MOS-450 monochromator, a PMS-250 photomultiplier detector, and an ALX-250 Xe and Xe/Hg arc lamp. The data shown in Fig. 6 were measured at 270 nm (the optimal wavelength for monitoring the production of CSSC) using a cell with a 1-cm pathlength. The solution velocities were 15 mL/s at the ball mixer. The data were analyzed using Bio-Logic software (Bio-Kine 32 V4.40), which is based upon the SIMPLEX algorithm.

Modeling of Kinetic Data

Figures 1 and 5 were computed using rate equations that were programmed into Mathematica 5.2. As explained previously [10], the simultaneous differential equations were solved by numerical methods. The essential part of the algorithm consisted of an iterative procedure that made use of the Euler–Cauchy method [12]. The Mathematica input files are available from the authors upon request.

RESULTS AND DISCUSSION

The Two Mathematical Models

The two mathematical models have been derived previously [10]. Model I is based upon the mechanism shown in Scheme 1:

$$\frac{d[CSH]^T}{dt} = -k_1[CS^-][H_2O_2] - k_2[CS^-][CSOH] \quad (1)$$

$$\frac{d[H_2O_2]}{dt} = -k_1[CS^-][H_2O_2] \quad (2)$$

$$\frac{d[CSOH]}{dt} = k_1[CS^-][H_2O_2] - k_2[CS^-][CSOH] \quad (3)$$

$$\frac{d[CSSC]}{dt} = k_2[CS^-][CSOH] \quad (4)$$

where

$$[CS^-] = \frac{[CSH]^T}{1 + \frac{[H^+]}{K_a}} \quad (5)$$

Although these ordinary differential equations (1)–(5), as previously explained in [10], do not have an analytical solution, they can be solved numerically using the Euler–Cauchy method [12]. This approach permits a direct comparison between model I and the simpler model we proposed (model II) for which $k_2[CS^-][CSOH] \gg k_1[CS^-][H_2O_2]$. Model II is defined by the following set of differential equations:

$$\frac{d[CSH]^T}{dt} = -2 \times k_1[CS^-][H_2O_2] \quad (6)$$

$$\frac{d[H_2O_2]}{dt} = -k_1[CS^-][H_2O_2] \quad (7)$$

$$\frac{d[CSSC]}{dt} = k_1[CS^-][H_2O_2] \quad (8)$$

When referring to model I, we are specifically referencing Eqs. (1)–(5), with the equilibrium constant $K_a = 10^{-8.44}$ M and the rate constants $k_1 = 15.2$ M^{-1} s^{-1} and $k_2 = 720$ M^{-1} s^{-1}, as proposed by Luo et al. [5]. For model II, we mean Eqs. (6)–(8) and the same constants (less k_2).

Attempts to Observe the Intermediate CSOH by ^{1}H NMR

For model I, some reaction conditions are predicted to produce substantial amounts of CSOH as a transient species. Figure 1 illustrates the computed time-resolved speciation of a reaction between CSH (4 mM) and H_2O_2 (9.2 mM), the conditions that were employed by Luo et al. to produce Fig. 3C of their original publication [5] and part of the data that were analyzed by Anderson and Luo in Table 1 of their subsequent reply [9] to our comment [10]. Figure 1, which illustrates the expected speciation of cysteine-derived species as predicted by model I, suggests that about 4% CSOH should form within 5 min of mixing. Without alternative reaction pathways (which are not specifically included in model I or II), about 4% CSOH is expected to remain at the end of the reaction. However, there are several possible reactions that could in principle consume the nascent RSOH, including its reaction with CSH to produce CSSC (which is modeled by the k_2 step

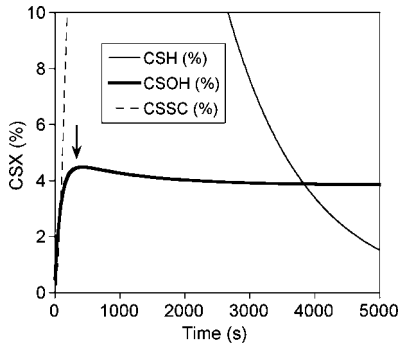

Figure 1 Simulation of the speciation of cysteine derivatives (CSX = CSH + CSOH + 2CSSC) as a function of time for model I: $[CSH]^T = [CSH] + [CS^-]$ (solid line), [CSOH] (bold line), and [CSSC] (dashed line) for the reaction of $[CSH]_0^T = 4$ mM and $[H_2O_2]_0 = 9.2$ mM at pH 6.0. This simulation predicts a steady-state concentration of ca. 4% CSOH will be achieved within the first 5 min of the reaction. The arrow indicates the point at which the ^{1}H NMR spectrum of Fig. 2 was measured.

of Scheme 1) and other reactions that are not included in the model of Scheme 1. Regarding unaccounted for reactions, for example, there exists the possibility of condensation to give the thiosulfinate ester (cystine *S*-monoxide, CS(=O)SC) and overoxidation to give the sulfinic acid (cysteine sulfinic acid, CSO_2H) and the sulfonic acid (L-cysteic acid, CSO_3H) (Scheme 2).

We have previously employed ^{1}H NMR spectroscopy to characterize the speciation of CSH, CSSC, CS(=O)SC, CSO_2^-, CSO_3^-, and related derivatives of CSH [11,13]. Regardless of the fate of CSOH, the existence of significant amounts of CSOH should leave telltale evidence in the ^{1}H NMR spectrum. In an effort to observe transient species, such as CSOH or CS(=O)SC (which is also unstable under these reaction conditions) [11], time-resolved ^{1}H NMR spectra were collected. Since a compromise was necessary whereby signal/noise (determined by the number of transients that were averaged) was limited by the need to collect periodic samples, the minimum number of transients that would be necessary to unambiguously establish the existence of 4% CSOH was first determined. For

Condensation

$$2\ CSOH \longrightarrow CS(=O)SC + H_2O$$

Oxidation

$$CSO_xH + H_2O_2 \longrightarrow CSO_{x+1}H + H_2O \quad x=1,2$$

Scheme 2 Representative reactions of cysteine sulfinic acid.

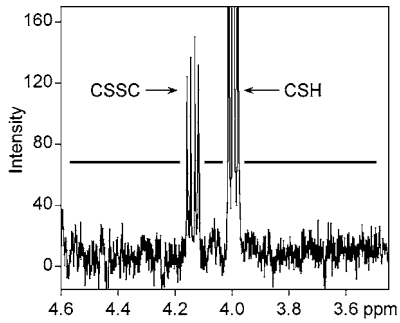

Figure 2 Time-resolved ^{1}H NMR spectrum for the oxidation of CSH (4 mM) by H_2O_2 (9.2 mM) to give CSSC. The H_α region of the ^{1}H NMR spectrum is illustrated after 5 min. A mixture of CSH (off scale) and CSSC is observed. The bar represents the expected height of the resonances for 4% CSOH (assuming a coupling pattern and linewidth for CSOH that is similar to that for CSH).

a 4 mM solution of CSH, it was established that an average of 16 transients was sufficient, which could be accomplished at intervals of 100 s. Figure 2 illustrates 1 of 50 spectra that were collected in increments of 100 s after the rapid mixing of a solution of CSH with a solution of H_2O_2 to give the final reaction mixture with the same concentrations as those that were employed during the simulation of Fig. 1. The first spectrum in this series was collected within 30 s of initiating the reaction. The spectrum in Fig. 2 illustrates the H_α region of the ^{1}H NMR spectrum after ca. 10% conversion of CSH to CSSC. The same point is marked in Fig. 1 with an arrow. The bar drawn across the spectrum of Fig. 2 illustrates the expected height of the doublet of doublets that would be anticipated for CSOH (assuming the same linewidth as that observed for CSH). There is no indication of the formation of CSOH or any of the products that might be derived from CSOH (e.g., CS(=O)SC, CSO_2^-, or CSO_3^-). After completion of the reaction (as evidenced by the complete conversion of CSH to CSSC), data collection was continued for eight additional hours, albeit with an increase in the number of transients averaged to 128. No additional change was observed in the spectra. There was no evidence of the aforementioned derivatives of CSOH in any of the spectra, except of course for CSSC.

Attempts to Observe the Intermediate CSOH by Electronic Spectroscopy

Previous efforts to monitor the reaction of CSH and H_2O_2 have included measuring the concentrations of CSH and H_2O_2 by colorimetric (e.g., by titrating unreacted CSH) and chromatographic methods. Electronic spectroscopy has apparently not been previously used to monitor the reaction, which is surprising given the

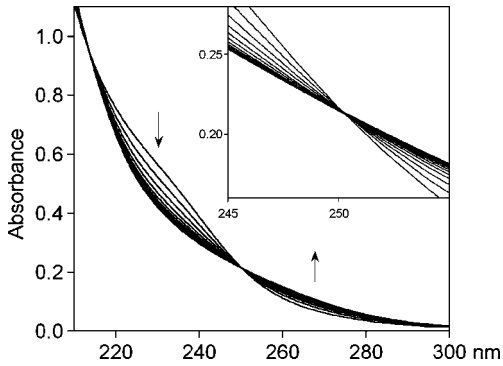

Figure 3 Time-resolved UV spectra for the reaction of CSH (5 mM) and H_2O_2 (50 mM) at pH 7.4 (150 mM phosphate buffer) at 22°C using a cell with a 1-mm pathlength. The temporal resolution was 1 (one third of the spectra are illustrated). Two isosbestic points are observed at 214 and 250 nm (the latter is illustrated in the inset). A band for CSH is observed disappearing synchronously with the time that a band for CSSC appears. Deconvolution of these spectra using SPECFIT produced the predicted spectra for CSH, H_2O_2, and CSSC (which were independently measured under the conditions of this experiment).

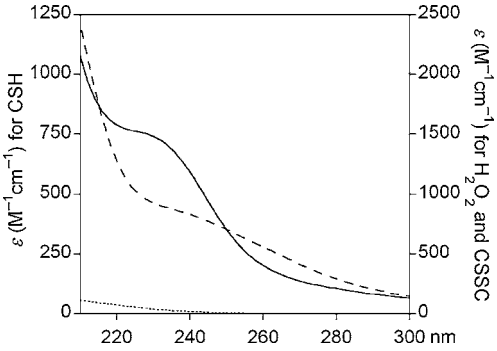

Figure 4 Electronic spectra of CSH (solid), H_2O_2 (short dashed), and CSSC (long dashed) at pH 7.4 (150 mM phosphate buffer). Two ordinate scales are used to reflect the stoichiometry of the reaction: $2CSH + H_2O_2 \rightarrow CSSC + H_2O$.

fact that the latter is less invasive than the methods that have thus far been employed. The electronic spectra of the reactants and products are sufficiently different that time-resolved electronic spectra that were collected during the course of the reaction could be deconvoluted using factor analysis of the three-dimensional data sets by singular value decomposition (SVD), vide infra. Typical time-resolved spectra are illustrated in Fig. 3. All of the time-resolved data sets that were collected, including the conditions of Figs. 1 and 2 (data not shown) as well as the conditions of Figs. 3 and 5, exhibit multiple isosbestic points. From independent measurements, it was established that the observed isosbestic points occur where the molar absorptivities of CSY and CSSC are equal (Fig. 4). Although the spectra of two distinguishable species frequently intersect to give an isosbestic point, it is extremely unlikely that the spectra of three or more distinguishable species will mutually coincide. So the stability of the isosbestic point is sound evidence that a reaction is proceeding without forming intermediates or multiple products that have significant absorbance at these points. Notably, SVD analysis of the data of Fig. 3 using model II yielded $k_1 = 14.62(8)\ M^{-1}\ s^{-1}$, which is comparable to literature values of this rate constant [5–8]. Analysis of the eigenvectors of the SVD analysis indicated only three colored species (which were confirmed to be CSH, H_2O_2, and CSSC). The deconvoluted spectra were identical to the spectra for CSH, H_2O_2, and CSSC, which were measured under identical conditions. These spectra are illustrated in Fig. 4 (cf. Fig. 3). Every effort to converge model I for the 5000 data points in the three-dimensional matrix failed. When k_2 was assigned an initial value of 720 $M^{-1}\ s^{-1}$ (the value reported by Luo et al.), SVD analysis produced a standard deviation that exceeded the value for k_2. No evidence was found for the existence of an intermediate in the time-resolved electronic spectra.

Attempts to Observe Pre–Steady-State Kinetics

As explained previously [10], the largest discrepancy between the two models will occur at the beginning of the reaction. Accordingly, attention is focused here on the initial rates, the first few percent of the reaction. Figure 5 depicts a simulation of the expected rates of formation of CSSC based upon the two models. Model I exhibits pre–steady-state behavior, as expected for a kinetically competitive k_2 step

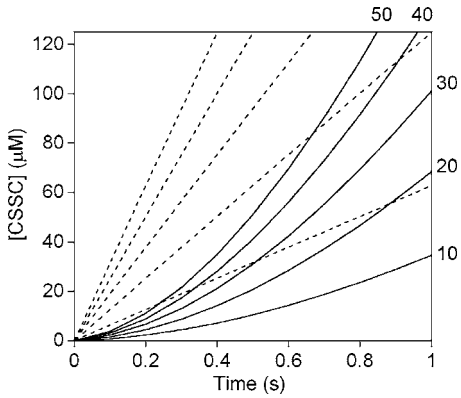

Figure 5 Simulation of the production of the first 5% of CSSC as a function of time for models I (solid lines) and II (dashed lines) for the reaction of $[CSH]_0^T = 5$ mM and $[H_2O_2]_0 = 10$–50 mM at pH 7.4. These plots illustrate the S-shaped induction period that is predicted by model I and the linear behavior that is predicted by model II (for initial-rate conditions).

before a steady-state concentration of the intermediate CSOH develops. In contrast, model II exhibits pseudo-zero-order kinetics during the initial rate period, since neither CSH nor H_2O_2 exhibits a significant change in concentration during the first 5% of the reaction. It is clear that the two models can be readily distinguished, provided the [CSSC] can be measured in the timeframe that is indicated (the millisecond timescale for the reaction conditions of Fig. 5). The short timescale of the reaction precludes the use of high performance liquid chromatography, which is the method that was employed by Luo et al. in their study [5]. However, electronic spectroscopy provides a convenient probe of the changing concentrations of CSSC. After investigating the entire spectrum, it was determined that the change in absorbance at 270 nm exhibited the greatest sensitivity to the formation of CSSC. Figure 6 illustrates the change in absorption at 270 nm that is observed during the first 5% of reaction of CSH with H_2O_2 under the same conditions that were employed to simulate the data of Fig. 5. It is clear that the observations of Fig. 6 are consistent with model II, and the linearity of the absorbance changes is inconsistent with model I. Since there is no apparent induction period and the magnitudes of the observed changes in absorption in Fig. 6 are as predicted by model II, it is concluded that a steady-state concentration of CSOH has been achieved during the mixing time of this experiment. For the measured deadtime of 1.6 ms for mixing, the half-life for the achievement of steady-state equilibrium must be less than 350 μs. Employing simulations analogous to those of Fig. 5, and in consideration of the signal/noise level of the data of Fig. 6, a *lower* limit of 10^5 M^{-1} s^{-1} is estimated for k_2.

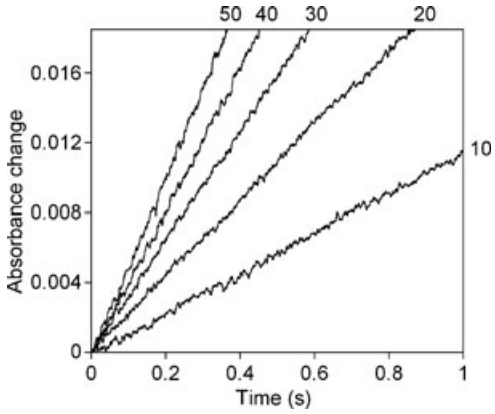

Figure 6 Observed increase in absorption at 270 nm for the reaction of $[CSH]_0^T = 5$ mM and $[H_2O_2]_0 = 10$–50 mM at pH 7.4. The same scale is employed for this graph as was used for Fig. 5.

CONCLUSION

A kinetic model that was proposed by Luo et al. for the oxidation of CSH by H_2O_2 vis-à-vis the transient species CSOH has been discredited [5]. Some of the methodological issues [9] that were raised during the recent exchange of ideas deserve comment. One reason that kinetics is routinely employed as a *formal* approach to studying chemical mechanisms is that it begins with a hypothesis. When the hypothesis and experiment are contrary, the former is modified and the procedure is iterated (i.e., the scientific method). Thus, it is said that kinetics can vanquish a postulated mechanism, but it can only, at best, support an alternative model. One cannot prove a chemical mechanism any more than one can prove any hypothesis that does not have an analytical solution. This is the approach that we have taken in the present study. Luo et al. have taken what is sometimes referred to as a "*nonformal*" approach in their application of kinetics to address a mechanistic question [5]. Furthermore, they have argued the advantage of such an approach [9]. Anderson et al. are not the first researchers to take this approach, and indeed there is a well-respected monograph by Schmid and Sapunov that expounds the merits of such a method, whereby the time dependence of concentration curves is treated as primary experimental data and as such are analyzed with the fewest assumptions [14]. According to Schmid and Sapunov, the nonformal kinetic method involves systematic (and typically exhaustive) analysis of kinetic traces. We believe the formal and nonformal kinetic methods are both valid approaches to address mechanistic problems. However, for the nonformal kinetic method, statistics should not be employed in investigations to eliminate hypotheses in lieu of systematic kinetic analysis [9]. Also, from a pragmatic perspective, we generally find the formal kinetic method (together with targeted experiments) to be a more efficient approach to address mechanistic questions.

BIBLIOGRAPHY

1. Pe'er, I.; Felder, C. E.; Man, O.; Silman, I.; Sussman, J. L.; Beckmann, J. S. Proteins: Struct Funct Bioinfo 2003, 54, 20–40.
2. Giles, G. I.; Tasker, K. M.; Collins, C.; Giles, N. M.; O'Rourke, E.; Jacob, C. Biochem J 2002, 364, 579–585.
3. Giles, G. I.; Tasker, K. M.; Jacob, C. Free Radical Biol Med 2001, 31, 1279–1283.
4. Giles, G. I.; Tasker, K. M.; Jacob, C. Gen Physiol Biophys 2002, 21, 65–72.
5. Luo, D.; Smith, S. W.; Anderson, B. D. J Pharm Sci 2005, 94, 304–316.

6. Winterbourn, C. C.; Metodiewa, D. Free Radical Biol Med 1999, 27, 322–328.
7. Barton, J. P.; Packer, J. E.; Sims, R. J. J Perkin Trans 2 1973, 1547–1549.
8. Radi, R.; Beckman, J. S.; Bush, K. M.; Freeman, B. A. J Biol Chem 1991, 266, 4244–4250.
9. Anderson, B. D.; Luo, D. J Pharm Sci 2006, 95, 19–24.
10. Ashby, M. T.; Nagy, P. J Pharm Sci 2006, 95, 15–18.
11. Nagy, P.; Ashby, M. T. Chem Res Toxicol 2005, 18, 919–923.
12. Coe, D. A. J Chem Educ 1987, 64, 496–497.
13. Ashby, M. T.; Aneetha, H. J Am Chem Soc 2004, 126, 10216–10217.
14. Schmid, R.; Sapunov, V. N. Monographs in Modern Chemistry, Vol. 14: Non-Formal Kinetics in Search for Chemical Reaction Pathways; Verlag Chemie: Weinheim, 1982.